Aging effect in paraelectric state of ferroelectrics: Implication for a microscopic explanation of ferroelectric deaging

Dezhen Xue,[1,2] Jinghui Gao,[1] Lixue Zhang,[1] Huixin Bao,[1,2] Wenfeng Liu,[1,2] Chao Zhou,[1,2] and Xiaobing Ren[1,2,a)]

[1]*Multi-disciplinary Materials Research Center and State Key Laboratory for Mechanical Behavior of Materials, Xi'an Jiaotong University, Xi'an 710049, People's Republic of China*

[2]*Ferroic Physics Group, National Institute for Materials Science, Tsukuba, 305-0047 Ibaraki, Japan*

(Received 3 June 2008; accepted 3 February 2009; published online 23 February 2009)

Most ferroelectric materials exhibit aging effect (a time-dependent change in physical properties) in their ferroelectric state; however, aging is not reported to exist in the paraelectric state. In this letter we report the existence of a "paraelectric aging effect" in Mn-doped $(Ba_{0.80}Sr_{0.20})TiO_3$ ceramics. We found that when the paraelectric state is formed from an aged ferroelectric state through a reverse ferroelectric transition, the paraelectric state shows a gradual increase in the dielectric permittivity and decrease in dielectric loss with time. Such paraelectric aging effect exists only in acceptor-doped samples, not in undoped samples. The kinetics of the paraelectric aging follows a simple relaxation function with activation energy of 0.43 eV. Our results suggest that the paraelectric aging stems from the migration of oxygen vacancies, being the same as the case of ferroelectric aging. We show that such a migration is driven by a symmetry-conforming short-range ordering tendency of point defects. Such a microscopic mechanism also provides a microscopic explanation for the well-observed "ferroelectric deaging effect." © *2009 American Institute of Physics*. [DOI: 10.1063/1.3086876]

For more than half a century, ferroelectric (FE) materials have been known to exhibit "aging effect" in FE state, i.e., a gradual change in physical properties with time.[1–6] As aging strongly affects the reliability of FE and dielectric devices, there is a constant interest in understanding its physical origin and in how to control it.

It is known that the FE aging effect can be eliminated by experiencing a heating to the paraelectric state, i.e., the so-called "FE de-aging effect."[7–9] However, it has remained unclear whether the "deaging" is caused by a mere transition into the paraelectric phase or by a diffusional process in the paraelectric phase. Common practice of deaging involves holding the sample in the paraelectric state for some time;[7–9] this seems to indicate that the FE deaging involves a time-dependent process in the paraelectric state, but its microscopic mechanism still remains obscure. On the other hand, it is generally agreed that FE aging is attributed to a gradual stabilization of the *FE domains* by defects.[2–7,10–12] Thus it is not clear whether or not there exists a time-dependent change in properties in the paraelectric state, where there exists neither spontaneous polarization nor domains.

In this letter we show clear evidence that there exists a time-dependent process in the paraelectric state during its aging, which we call "paraelectric aging," in contrast to the well-known "FE aging" in the FE state. We show that the paraelectric phase of a simple perovskite FE, Mn-doped $(Ba_{0.80}Sr_{0.20})TiO_3$ (BST) ceramic, shows a gradual change in the dielectric permittivity (ε) and loss ($\tan\delta$) with time. Such paraelectric aging occurs only in acceptor-doped samples and when the paraelectric state is formed from an *aged* FE state. We further suggest that the mechanism is the symmetry-conforming short-range ordering (SC-SRO) tendency of defects, similar to that for FE aging.[5–7] Finally, we show that such a time-dependent paraelectric aging process and its mechanism provide a natural explanation for the long-standing FE de-aging effect.

The samples were 1%Mn doped $(Ba_{0.80}Sr_{0.20})TiO_3$ ceramics (abbreviated as BST-1Mn). Mn^{3+} was added as acceptor dopant,[13] and oxygen vacancies are simultaneously created by charge compensation. Sr^{2+} was added to lower the Curie temperature to about 57 °C (Ref. 14) so that the paraelectric aging is not too fast to detect. Acceptor-free BST samples were also fabricated for comparison. All the samples were prepared by a conventional solid-reaction method. Paraelectric aging was performed in an oil bath with a temperature fluctuation of less than 0.1 °C. The measuring frequency was 100 Hz and the ac signal level was 1 V for all the samples. The noise level of permittivity was less than ±0.05%.

We first explore the paraelectric aging effect for a BST-1Mn sample. The sample was aged at 30 °C ($<T_c$) for a week. Then the sample was up-quenched to an oil bath fixed at 90 °C ($=T_c+33$ °C) to transform into a paraelectric phase. At the same time we started to measure dielectric permittivity (ε) and dielectric loss ($\tan\delta$) as a function of aging time in the paraelectric state. Contrary to the general expectation that paraelectric state should be a stable state, Fig. 1 shows clearly that the dielectric permittivity and dielectric loss vary with increasing aging time in the paraelectric state (at 90 °C). Dielectric permittivity exhibits a gradual increase with time and saturates at a value about 2.0% higher than its initial value [Fig. 1(a)]; in the meantime, the dielectric loss shows a gradual decrease and finally saturates at a value about 2.5% lower than its initial one [Fig. 1(b)]. Therefore, aging effect indeed exists in the paraelectric state of FE materials.

a)Author to whom correspondence should be addressed. Electronic mail: ren.xiaobing@nims.go.jp.

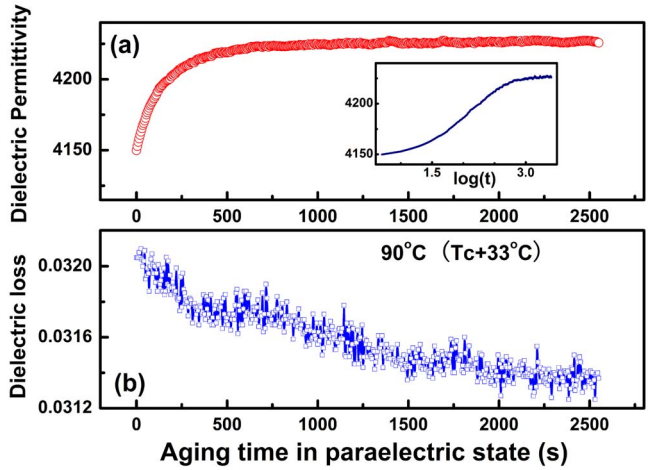

FIG. 1. (Color online) Evidence for the paraelectric aging effect of BST-1Mn. (a) Dielectric permittivity $\varepsilon(t)$ and (b) dielectric loss tan $\delta(t)$ show gradual change with time t. The inset shows that paraelectric aging does not follow the empirical linear relation between $\varepsilon(t)$ and $\log(t)$.

To clarify the origin of the unexpected paraelectric aging effect, we first explored the possibility that the paraelectric aging effect may be related to a specific metastable "microscopic state" of the paraelectric phase. For this purpose, we compared the paraelectric aging behavior of two "different paraelectric states" of the same paraelectric BST-1Mn. One paraelectric state is formed by a quick reverse transition from *an aged FE state* (i.e., with prior aging in the FE state); the other is formed by a quick reverse transition from *an unaged FE state* (i.e., without prior aging in the FE state). As shown in Fig. 2(a), the paraelectric state with prior FE aging shows a gradual increase in the dielectric permittivity with time, i.e., a paraelectric aging effect. By contrast, the paraelectric state without prior FE aging shows no paraelectric aging effect. Such contrasting behavior reveals that the paraelectric aging stems from a special microscopic state, which is inherited from the aged FE state.

We further explore the relation between paraelectric aging and point defects. Figure 2(b) shows that point defects indeed play a crucial role in the paraelectric aging effect. The acceptor-free sample ($0.0\%Mn^{3+}$) shows a negligible paraelectric aging, but the acceptor-doped sample ($1.0\%Mn^{3+}$) shows clear paraelectric aging. Therefore, the

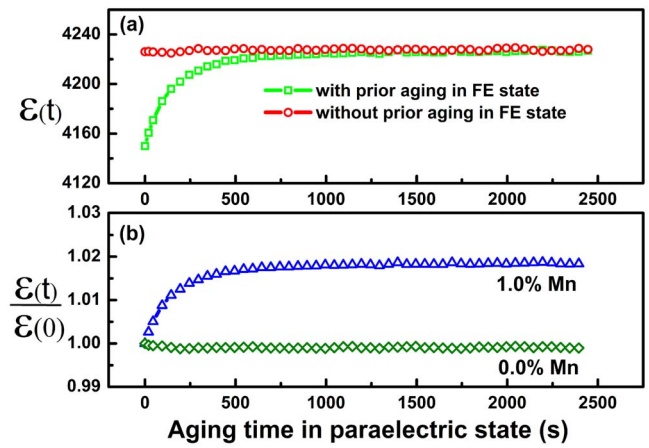

FIG. 2. (Color online) (a) Different paraelectric aging behavior of BST-1Mn with and without prior FE aging at 90 °C. The prior FE aging treatment was at 30 °C for 1 week. (b) Effect of acceptor defect (Mn^{3+}) on the paraelectric aging effect. $\varepsilon(t)/\varepsilon(0)$ is relative change in permittivity.

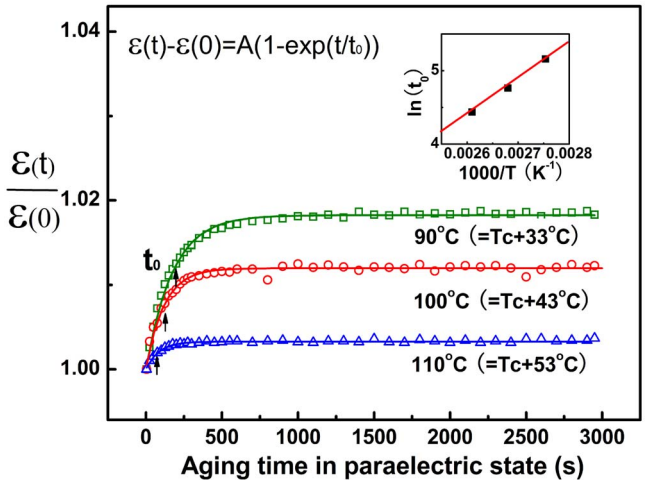

FIG. 3. (Color online) The paraelectric aging effect at different temperatures. All the dielectric permittivity behaviors fit well to a relaxation function $\varepsilon(t)-\varepsilon(0)=A[1-\exp(t/t_0)]$, where $A[=\varepsilon(\infty)-\varepsilon(0)]$ is the magnitude of the aging effect and the relaxation time t_0 is a measure of the aging rate. Arrows indicate the relaxation time t_0. $\varepsilon(0)$ at 90, 100, and 110 °C are 4150, 3525, and 2890, respectively. The inset shows the Arrhenius plot of $\ln(t_0)$ vs $1/T$.

existence of point defects, i.e., the acceptor dopant and the induced oxygen vacancies, is a necessary condition for the paraelectric aging effect.

To explore the microscopic process during paraelectric aging, the kinetics of paraelectric aging at different temperatures was studied for the BST-1Mn sample, and the result is shown in Fig. 3. It is clear that the aging behavior is qualitatively the same for different aging temperatures, but the aging becomes faster with increasing aging temperature. We found for all aging temperatures that the dielectric permittivity fits well to a simple relaxation function, $\varepsilon(t)-\varepsilon(0)=A[1-\exp(t/t_0)]$, where t_0 is the relaxation time and $\varepsilon(0)$ is the initial permittivity value. From the arrow positions (t_0 values) in Fig. 3, it is clear that the relaxation time decreases with increasing aging temperature. The $\ln(t_0)$ versus $1/T$ Arrhenius plot yields a low activation energy of 0.43 eV (inset of Fig. 3). This activation energy value is close to the recently reported values for acceptor-doped $BaTiO_3$ (Ref. 15) but is lower than those in earlier studies.[16] The reason for such a discrepancy may be due to different physical processes under investigation.

Here comes the central question: what is the driving force for the migration of point defects? Before answering this question, we note an important clue from Fig 2(a): *the paraelectric aging is closely related to the prior aging in the FE state*. This important fact indicates that the origin of paraelectric aging is linked to the origin of FE aging. For FE aging effect, recent studies[5–7,10,11] have shown that the FE aging stems from a "SC-SRO" of point defects.[17,18] In the following we shall show that the paraelectric aging comes from the same SC-SRO tendency.

The main idea of the SC-SRO principle is that the symmetry of SRO distribution of point defects tends to follow the crystal symmetry when in equilibrium.[6,17,18] We consider a typical ABO_3 structure to explain the symmetry property of point defects and the paraelectric aging effect (Fig. 4). Here only the symmetry of the statistical distribution of O^{2-} vacancies around a defect ion Mn^{3+} is concerned. After aging in the FE state, according to the SC-SRO principle the SRO

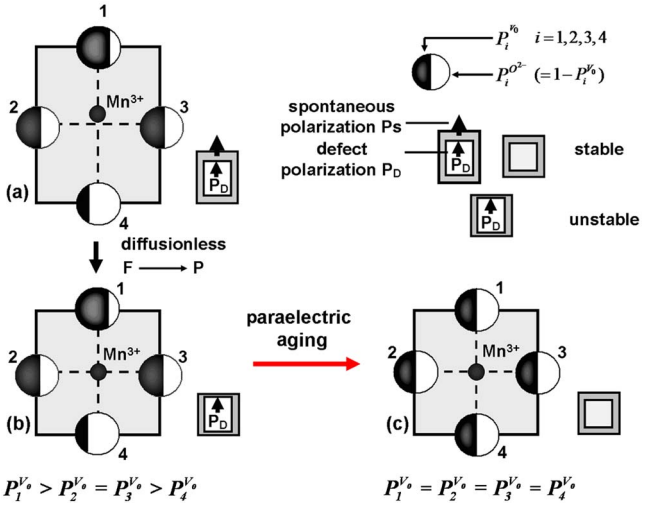

FIG. 4. (Color online) Microscopic mechanism of the paraelectric aging effect. For simplicity, the (100) plane of the perovskite structure is shown. (a) Aged FE state where defect symmetry around an acceptor ion (Mn^{3+}) is tetragonal. (b) Cubic crystal symmetry immediately after transition in which the defect symmetry around an acceptor ion (Mn^{3+}) remains a polar tetragonal symmetry (with a defect polarization $\mathbf{P_D}$). (c) Equilibrium cubic state after aging (diffusion) in the paraelectric state in which both the defect symmetry and the crystal symmetry are cubic. $P_i^{V_O}$ is the conditional probability of finding an oxygen vacancy at sites (1–4) around an acceptor ion (Mn^{3+}). The large rectangle/square and small rectangle/square denote crystal symmetry and defect SRO symmetry, respectively.

distribution of O^{2-} vacancies around a Mn^{3+} dopant follows the polar tetragonal crystal symmetry, and such a distribution forms a defect polarization $\mathbf{P_D}$ along the direction of $\mathbf{P_S}$,[6,19,20] as shown in Fig. 4(a). When the transition from FE to paraelectric occurs, the tetragonal crystal symmetry changes abruptly to the cubic symmetry, but SRO defect symmetry cannot follow such an abrupt change because a change in defect symmetry would require the exchange ions/vacancies (i.e., diffusion), which is forbidden during the diffusionless transition. As a result, the initial microscopic state of the paraelectric phase immediately after the transition is a noncentric tetragonal distribution of oxygen vacancies around Mn^{3+} in a cubic paraelectric lattice [Fig. 4(b)]. This state is equivalent to a cubic paraelectric phase embedded with an internal polarization $\mathbf{P_D}$ created by the point defects.

The defect polarization $\mathbf{P_D}$ in the paraelectric state gives rise to an internal dc bias field $\mathbf{E_D}=\mathbf{P_D}/\varepsilon_0\chi$, where ε_0 and χ are the vacuum permittivity and electric susceptibility, respectively. This internal field $\mathbf{E_D}$ is equivalent to a dc bias field; thus the effect of paraelectric aging on dielectric permittivity and dielectric loss can be understood by considering how this internal field $\mathbf{E_D}$ changes with aging time and consequently changes the permittivity and loss.

Since the paraelectric state formed from an aged FE state is a cubic paraelectric phase with a noncubic SRO defect symmetry [Fig. 4(b)], it is unstable according to the SC-SRO principle; thus it tends to change into a stable state in which the defect symmetry is also cubic [Fig. 4(c)]. This is achieved through the paraelectric aging process. During the paraelectric aging [Figs. 4(b) and 4(c)], point defects gradually rearrange themselves into a cubic distribution through short-range diffusion, i.e., oxygen vacancy $V^{O^{2-}}$ migrates from site 1 to 2, 3, or 4 until making the four sites have the same SRO parameter [Fig. 4(c)]. As the consequence, the internal field $\mathbf{E_D}$ produced by $\mathbf{P_D}$ gradually diminishes during aging. As the effect of a dc bias field E on permittivity is given by[21] $\varepsilon(E)=\varepsilon_1-\varepsilon_2\cdot E^2+o(E^2)$ (where ε_1 and ε_2 are positive constants and $o(E^2)$ includes all higher order terms), the permittivity gradually increases from the unaged paraelectric state (with the maximum $\mathbf{E_D}$) and finally reaches the well-aged paraelectric state (with $\mathbf{E_D}=0$) during aging. The decrease in dielectric loss ($\tan\delta$) during paraelectric aging can also be considered as being caused by the gradual decrease in the dc bias field $\mathbf{E_D}$ from the relation $\tan\delta=\tan\delta_0+\omega B\varepsilon^5E^2$ (where $\tan\delta_0$ is the field-independent dielectric loss, ω is the frequency, B is a constant, and ε is the permittivity).[22]

It should be noted that the paraelectric aging effect is fundamentally different from another defect-induced effect in the paraelectric state—the Burn's effect,[23] i.e., the formation of nanosized polar (FE) regions in a paraelectric matrix due to the presence of static point defects. Burn's effect is a time-independent effect, contrary to the time dependence of the paraelectric aging effect.

Finally, it should be pointed out that the paraelectric aging process explains the longstanding puzzle why a "deaging treatment" can remove the *prior FE aging effect*. Figure 4 clearly shows that the microscopic mechanism for deaging is that the polar defect SRO symmetry formed by FE aging is "corrected" into the cubic defect SRO symmetry during paraelectric aging. This results in the rejuvenation to the "normal" FE state upon subsequent cooling through T_c, and thus the FE aging effect disappears.[5,6] Therefore, the FE deaging requires both FE transition and a diffusional process in paraelectric state.

This work was supported by Kakenhi of JSPS, the National Basic Research Program of China (Grant No. 2004CB619303), and the 111 Project of China.

[1] K. Uchino, *Ferroelectric Device* (Dekker, New York, 2000).
[2] W. A. Schulze and K. Ogino, Ferroelectrics **87**, 361 (1988).
[3] U. Robels and G. Arlt, J. Appl. Phys. **73**, 3454 (1993).
[4] G. Arlt and H. Neumann, Ferroelectrics **87**, 109 (1988).
[5] L. X. Zhang and X. Ren, Phys. Rev. B **73**, 094121 (2006).
[6] X. Ren, Nature Mater. **3**, 91 (2004).
[7] L. X. Zhang and X. Ren, Phys. Rev. B **71**, 174108 (2005).
[8] M. C. McQuarrie and W. R. Buessem, Am. Ceram. Soc. Bull. **34**, 402 (1955).
[9] W. A. Schulze and J. V. Biggers, Ferroelectrics **9**, 203 (1975).
[10] M. M. Ahmad, K. Yamada, P. Meuffels, and R. Waser, Appl. Phys. Lett. **90**, 112902 (2007).
[11] D. Lin, K. W. Kwok, and H. L. W. Chan, Appl. Phys. Lett. **90**, 232903 (2007).
[12] Y. A. Genenko and D. C. Lupascu, Phys. Rev. B **75**, 184107 (2007).
[13] A. A. Kirianov, N. Ozaki, H. Ohsato, N. Kohzu, and H. Kishi, Jpn. J. Appl. Phys., Part 1 **40**, 5619 (2001).
[14] F. Jona and G. Shirane, *Ferroelectric Crystals* (MacMillan, New York, 1962).
[15] S. H. Cha and Y. H. Han, J. Appl. Phys. **100**, 104102 (2006).
[16] O. Bidault, P. Goux, M. Kchikech, M. Belkaoumi, and M. Maglione, Phys. Rev. B **49**, 7868 (1994).
[17] X. Ren and K. Otsuka, Nature (London) **389**, 579 (1997).
[18] X. Ren and K. Otsuka, Phys. Rev. Lett. **85**, 1016 (2000).
[19] K. A. Müller, W. Berlinger, and J. Albers, Phys. Rev. B **32**, 5837 (1985).
[20] R.-A. Eichel, P. Erhart, P. Traskelin, K. Albe, H. Kungl, and M. J. Hoffmann, Phys. Rev. Lett. **100**, 095504 (2008).
[21] C. Ang and Z. Yu, Phys. Rev. B **69**, 174109 (2004).
[22] G. Rupprecht, R. O. Bell, and B. D. Silverman, Phys. Rev. **123**, 97 (1961).
[23] G. Burns and F. H. Dacol, Phys. Rev. B **28**, 2527 (1983).